doi:10.1016/j.jmb.2005.11.052 J. Mol. Biol. (2006) 356, 432–443

JMB

Available online at www.sciencedirect.com

SCIENCE DIRECT®

ELSEVIER

# GTP-dependent Formation of a Ribonucleoprotein Subcomplex Required for Ribosome Biogenesis

**Katrin Karbstein[1] and Jennifer A. Doudna[1,2,3]***

[1]*Department of Molecular and Cell Biology, University of California at Berkeley, Berkeley CA 94720-3206, USA*

[2]*Department of Chemistry University of California at Berkeley, Berkeley, CA 94720-3206, USA*

[3]*Howard Hughes Medical Institute, University of California at Berkeley, Berkeley CA 94720-3206, USA*

**Corresponding author*

Ribosome biogenesis in eukaryotic organisms involves the coordinated assembly of 78 ribosomal proteins onto the four ribosomal RNAs, mediated by a host of *trans*-acting factors whose specific functions remain largely unknown. The essential GTPase Bms1, the putative endonuclease Rcl1 and the essential U3 small nucleolar RNA form a stable subcomplex thought to control an early step in the assembly of the 40 S ribosomal subunit. Here, we provide a complete thermodynamic analysis of GTP-dependent subcomplex formation, revealing strong thermodynamic coupling of Rcl1, U3 small nucleolar RNA and GTP binding to Bms1 that is eliminated in the presence of GDP. The results suggest that Rcl1 activates Bms1 by promoting GDP/GTP exchange, analogous to ribosome-promoted nucleotide exchange within translation elongation factor EF-G. These and other data unveil thermodynamic similarities between Bms1 and the subgroup of GTPases involved in translation, providing evidence that parts of the ribosome assembly machinery may have evolved from the translation apparatus. This quantitative description of an early and essential step in pre-ribosome assembly provides a framework for elucidating the network of interactions between the Bms1 subcomplex and additional factors involved in ribosome biogenesis.



*Keywords:* ribosome; GTPase; RNA; pre-ribosome assembly; ribosome biogenesis

## Introduction

Ribosomes are synthesized in eukaryotes through the coordinated action of dozens of small RNAs as well as >170 *trans*-acting protein factors.[1] Together, these players orchestrate methylation of specific 2′-hydroxyl groups and modification of certain uridine bases, as well as RNA cleavage reactions, folding of the rRNA and binding of the ribosomal proteins (Figure 1(a)). While the identities of most factors involved in ribosome biogenesis have been discovered, their molecular functions remain largely uncharacterized. Genetic experiments and direct biochemical purification revealed that a large complex, termed the small subunit (SSU) processosome, is recruited to pre-rRNA *via* interactions with U3 small nucleolar RNA (snoRNA).[2,3] U3 snoRNA, an essential RNA that is conserved from yeast to humans, contains sequences complementary to those of 18 S rRNA and pre-rRNA. While it has been known from genetic and biochemical experiments for almost 20 years that the U3 snoRNA must anneal to pre-rRNA, its exact role in ribosome biogenesis is not clear. Apart from U3 snoRNA, the SSU processosome contains at least 31 proteins, including several RNA-binding proteins, an RNA helicase and a putative ATPase.[2,3] Conspicuously absent are endonucleases required for the RNA cleavage steps needed for 40 S subunit biogenesis.

The phylogenetically conserved protein Bms1, a component of the SSU processosome, is the only known GTPase required for 40 S subunit assembly. Both its GTP hydrolytic activity and its genetically defined interaction with 14-3-3 proteins,[4] which are adaptors of phosphorylation-controlled signaling, suggest that Bms1 is an important regulator of ribosome biogenesis. Previous work has shown that Bms1, together with the putative endonuclease Rcl1, binds to U3 snoRNA to form a stable subcomplex within the SSU processosome.[3,5–7] Additional biochemical and *in vivo* experiments

Abbreviations used: SSU, small subunit of the ribosome; GMPPNP, guanosineimidodiphosphate; TLC, thin-layer chromatography; snoRNA, small nucleolar RNA.

E-mail address of the corresponding author: doudna@berkeley.edu

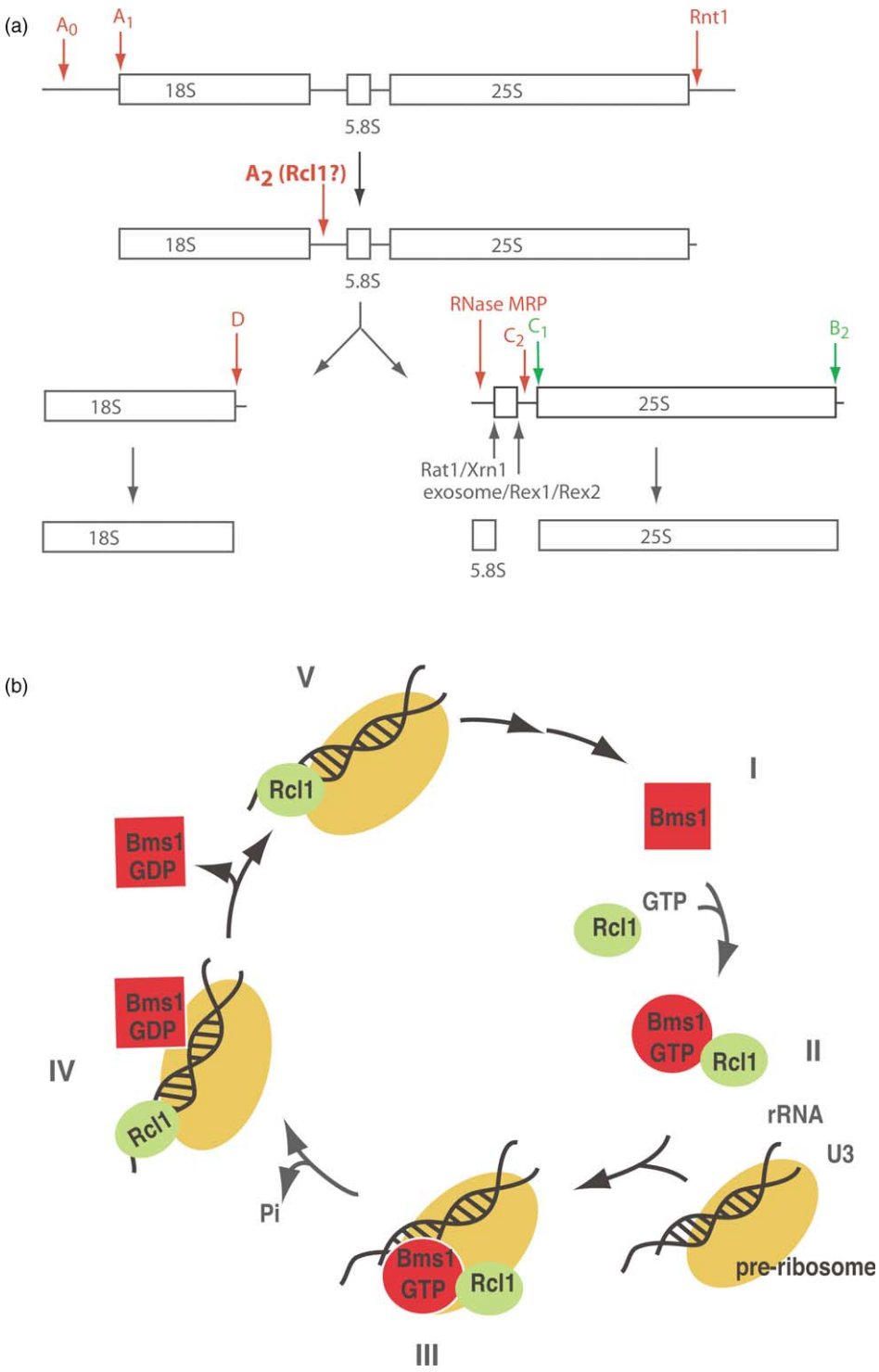


**Figure 1.** (a) Simplified representation of the pre-rRNA processing pathway (adapted from Venema & Tollervey).[41] Cleavage steps by endonucleases are shown in red, processing steps by exonucleases are shown in black, and steps where it is not known whether they are executed by endo- or exonucleases are shown in green. Pre-rRNA processing is initiated by Rnt1 cleavage at the 3′-end of the transcript. This is followed by cleavage at sites $A_0$ and $A_1$ by unknown endonucleases. Cleavage at site $A_2$ has been suggested to be performed by Rcl1,[42] and results in separation of the RNAs for the small and large subunits. The 18 S maturation is finalized by cleavage at site D in the cytoplasm, while maturation of 5.8 S and 25 S occurs in multiple steps in the nucleus. In all, 85% of transcripts are cleaved by RNase MRP before being processed by the Rat1/Xrn1 complex and at site $B_2$. This is followed by cleavage at sites $C_1$ and $C_2$, and processing by Rex1/Rex2[43] and the exosome to generate mature 5.8 S RNA. In the remaining 15% of transcripts, RNase MRP cleavage does not occur. (b) Bms1 delivers Rcl1 to pre-ribosomes. Bms1 is shown in red, Rcl1 is shown in green. Pre-ribosomes are shown in orange and U3 is shown in a duplex with pre-rRNA. The ternary complex of Bms1·GTP and Rcl1 binds tightly to U3 RNA, which is bound to pre-rRNA, locating the complex to pre-ribosomes. GTP hydrolysis leads to dissociation of Rcl1 and subsequent dissociation of Bms1 from U3 snoRNA.

provided evidence for a model in which Bms1-catalyzed GTP hydrolysis controls the delivery of Rcl1 to pre-ribosomes (Figure 1(b)).[7]

This proposed function of Bms1 resembles that of other GTPases that act as molecular switches to regulate specific biological pathways.[8] In particular, several GTPases are among the essential translation factors that control initiation, elongation and release of proteins synthesized by the ribosome, including elongation factors G and Tu, initiation factor 2 and release factor 3. Similar to other GTPases, GTP and effector binding is thermodynamically coupled for these translation factors,[9,10–16] and their GTPase activity is accelerated by several orders of magnitude upon interaction with a common site on the large (60 S) ribosomal subunit.[17–23] GTP hydrolysis is then used to render irreversible a step in protein synthesis that would otherwise be at equilibrium. In each case that has been studied in detail, the kinetic and thermodynamic behavior of the GTPase reflects its biological activities and enables comparison to other GTPase-controlled events.

To determine how GTP binding and hydrolysis affects the assembly of the Bms1·Rcl1·U3 snoRNA subcomplex, we determined the thermodynamic parameters of Bms1 binding to U3 snoRNA, Rcl1 and GDP or the non-hydrolyzable GTP analog GMPPNP. This analysis reveals significant similarities between the behavior of Bms1 and that of GTPases involved in translation, suggesting an evolutionary origin of Bms1 in the translational apparatus. Our results provide the first complete thermodynamic description of a critical early event in the assembly of the pre-ribosomal processing machinery, an important step towards understanding the complexities of ribosome biogenesis.

## Results

Quantitative thermodynamic analysis can provide important information about how complexes are assembled and stabilized. Furthermore, analysis of thermodynamic cycles can provide detailed functional information of networks of molecular interactions.[10,24–33] To probe the biochemical activities of ribosome assembly factors, we have focused on an essential subcomplex within the SSU processosome responsible for 40 S ribosomal subunit biogenesis. Previous work identified the essential GTPase Bms1 and the putative endonuclease Rcl1 as interacting partners within the SSU processosome.[3,5–7] Additional prior work has shown that Bms1 also directly binds to U3 snoRNA.[7] To determine how GTP binding and hydrolysis influence the binding and dissociation of Bms1 and its binding partners Rcl1 and U3 snoRNA, we carried out a complete thermodynamic analysis of this tripartite complex, in the presence of GDP and in the presence of the GTP analog GMPPNP. The resulting thermodynamic framework was constructed using kinetic data from GTPase experiments as well as RNA-binding experiments using nitrocellulose filter retention.

As described,[7] full-length Bms1 (136 kDa, 1183 amino acid residues) is poorly over-expressed and hydrolyzed efficiently, producing an N-terminal proteolysis fragment that comprises about two-thirds of the protein. In contrast, a truncated construct containing amino acid residues 1–705 designed according to the observed size and sequence of the major proteolysis fragment could be expressed stably as an N-terminal maltose-binding protein (MBP) fusion protein in *Escherichia coli*. This protein retains the binding sites for Rcl1 and U3 snoRNA,[7] and was used for the experiments described here. Control experiments confirmed that the MBP-tag does not affect binding of Rcl1 and U3 snoRNA.[7] Furthermore, we have shown that the GTPase activity and nucleotide binding responds to mutations within Bms1, demonstrating that GTPase hydrolysis is catalyzed by Bms1 and not a contaminant.[7]

### Thermodynamic framework for binding of GDP, Rcl1 protein and U3 snoRNA to Bms1

#### *Binding of GDP to Bms1, Bms1·Rcl1, Bms1·U3 and Bms1·U3·Rcl1*

To test whether binding of GDP, Rcl1 protein and U3 snoRNA to Bms1 are thermodynamically coupled events, which would indicate that a structural network links these ligand-binding sites, we determined the GDP affinity for free Bms1 as well as that for Bms1·Rcl1, Bms1·U3 and Bms1·Rcl1·U3.

Single-turnover GTPase experiments were used to determine the GDP affinity of Bms1-containing complexes *via* inhibition experiments. Under conditions where Bms1 is sub-saturating with respect to GTP, the concentration of GDP at which 50% inhibition is observed corresponds to the binding constant for GDP, $K_d^{GDP}$, as described in Materials and Methods. To measure the affinity of GDP for Bms1·Rcl1, Bms1·U3 and Bms1·Rcl1·U3, the respective complexes were pre-formed by the addition of saturating excess concentrations of Rcl1 protein and/or U3 snoRNA. The results of these experiments are summarized in Table 1, where it is revealed that U3 snoRNA as well as Rcl1 binding has little or no effect on GDP binding to Bms1.

#### *Binding of U3 snoRNA to Bms1, Bms1·GDP, Bms1·Rcl1 and Bms1·Rcl1·GDP*

To confirm the observation that there is little cooperativity in the presence of GDP, we determined the affinity of U3 snoRNA for Bms1, Bms1·GDP and Bms1·Rcl1·GDP (as well as for Bms1·Rcl1) in filter-binding experiments, as described in Materials and Methods. The data in Table 2 confirm that there is little thermodynamic coupling between binding of GDP and U3 snoRNA

**Table 1.** Nucleotide affinities from GTPase experiments

| | $K_i$ (μM) | | | | |
|---|---|---|---|---|---|
| | GDP | Ratio | GMPPNP | Ratio | $K_i^{GDP}/K_i^{GMPPNP}$ |
| Bms1 | 22±10[a] | (1) | 182±88[a] | (1) | 0.1 |
| Bms1·U3 | 54±21 | 2.5 | 428±110 | 2.6 | 0.1 |
| Bms1·Rcl1 | 14±7[a] | 0.6 | 14±8[a] | 0.08 | 1 |
| Bms1·Rcl1·U3 | 27±8 | 1.2 | 3.4±2 | 0.02 | 7.9 |

All measurements were made at 30 °C, 200 mM KCl, 10 mM $MgCl_2$, 50 mM Hepes (pH 7.7). Binding affinities were determined in single-turnover inhibition experiments as described in Materials and Methods. Binding affinities are averages of at least three independent experiments.
[a] As determined previously.[7]

to Bms1 ($K_d$ = 0.6 μM and 0.7 μM for binding of U3 snoRNA to Bms1 and Bms1·Rcl1, respectively.). Taken together, the lack of thermodynamic coupling in binding of GDP, Rcl1 and U3 snoRNA to Bms1 suggests that extended networks of interactions linking the binding sites for these ligands on Bms1 do not exist.

## Thermodynamic framework for binding of GMPPNP, Rcl1 protein and U3 snoRNA to Bms1

### *Binding of GMPPNP to Bms1, Bms1·Rcl1, Bms1·U3 and Bms1·U3·Rcl1*

We next wanted to test whether there are interactions between the binding sites for Rcl1 and U3 snoRNA in the GTP-bound state of Bms1. This state was probed using the non-hydrolyzable GTP analog GMPPNP. To do this, we determined whether there was thermodynamic coupling in the binding of ligands by comparing GMPPNP affinities in the presence and in the absence of Rcl1 and/or U3 snoRNA to test whether Rcl1 (or U3 snoRNA) binding enhances the affinity of Bms1 for GMPPNP. The affinities for the GTP analog GMPPNP were determined in inhibition experiments as described above for GDP and in more detail in Materials and Methods. These data are summarized in Table 1. In contrast to binding of GDP, binding of GMPPNP shows strong cooperativity with binding of U3 snoRNA and Rcl1. Binding of GMPPNP is strengthened 13-fold by addition of Rcl1 and another fourfold by addition of U3 RNA, leading to >50 fold stronger binding of GMPPNP to Bms1·Rcl1·U3 compared to Bms1 alone (Table 1). Comparison of the affinities for GMPPNP and GDP to that of free Bms1 shows that Bms1 binds GDP almost tenfold more strongly than GMPPNP, while this ratio is reversed in the Bms1·Rcl1·U3 complex (Table 1). Additionally, slight (about twofold) anticooperativity is observed between binding of U3 snoRNA and GMPPNP, in the absence of Rcl1.

**Table 2.** U3 snoRNA affinities of different Bms1 complexes

| | $K_d$ (μM) | |
|---|---|---|
| | Bms1 | Bms1·Rcl1 |
| Free | 1.0±0.4 | 0.6±0.3 |
| GDP | 1.5±0.5[a] | 0.7±0.2[a] |
| GMPPNP | 2.2±1.7[a] | 0.4±0.2[a] |

Binding affinities were determined in filter-binding experiments at 30 °C, 10 mM $MgCl_2$, 200 mM KCl and 50 mM Hepes (pH 7.7) as described in Materials and Methods. Binding affinities are the averages of at least three independent experiments.
[a] As determined previously.[7]

## Binding of U3 snoRNA to Bms1, Bms1·GMPPNP, Bms1·Rcl1 and Bms1·Rcl1·GMPPNP

To confirm the observed cooperativity between binding of GMPPNP and U3 snoRNA and Rcl1 to Bms1, we determined the affinity of Bms1, Bms1·GMPPNP and Bms1·Rcl1·GMPPNP for U3 snoRNA. The small amount of cooperativity between binding of Rcl1, U3 snoRNA and GMPPNP to Bms1 was verified in RNA-binding experiments, where binding of U3 snoRNA to Bms1·GMPPNP·Rcl1 is tighter than binding to Bms1·Rcl1 ($K_d$ = 0.6 μM and 0.4 μM†, for binding to Bms1·Rcl1 and Bms1·Rcl1·GMPPNP, respectively, Table 2). Additionally, the slight anticooperativity in binding of GMPPNP and U3 snoRNA to free Bms1 was observed also with binding of U3 snoRNA to free Bms1 being about twofold tighter ($K_d$ = 1.0 μM and 2.2 μM, Table 2).

The cooperativity in binding of GMPPNP (or GTP), Rcl1 and U3 snoRNA to Bms1 suggests the presence of structural contacts linking these binding sites. Analogous to other GTPases, we suggest that binding of GMPPNP (or GTP) rearranges the switch regions,[34] which also contact the binding site for Rcl1 and possibly U3 snoRNA.

## Direct determination of the affinity of Bms1·Rcl1·U3 for GTP

The inhibition experiments described above show that binding of GMPPNP to Bms1·Rcl1·U3

† The value of 0.4 μM for binding of U3 to Bms1·Rcl1·GMPPNP may be a lower limit, because full equilibration of this complex may have been prevented as Bms1 protein becomes inactive over the very slow time course of U3 dissociation ($k_{off}$ = 0.01 $min^{-1}$, in the absence of Rcl1 and GMPPNP, data not shown).

is strong, with an affinity of 3.4 μM. Assuming a similar affinity for GTP and GMPPNP, GTP binding should be measurable directly by monitoring the rate constant for GTP hydrolysis as a function of increasing concentrations of Bms1·Rcl1·U3, with GTP supplied in trace amounts. This experiment relies on equilibration of GTP-binding being fast relative to GTP hydrolysis. Because of weak binding of GTP and slow GTP hydrolysis, this assumption appears to hold true, as discussed below (Binding of Rcl1 to Bms1 and Bms1·U3; Figure 4).

To measure GTP binding to Bms1·Rcl1·U3 snoRNA, we pre-formed the Bms1·Rcl1·U3 complex by incubating Bms1 with excess, saturating concentrations of Rcl1 and U3 RNA prior to starting the GTPase reaction by the addition of GTP. The data in Figure 2(a) show that, as predicted, the rate constant for GTP hydrolysis of Bms1·Rcl1·U3 levels off, with an apparent $K_{1/2}$ of 6.3 μM, consistent with the inhibition data presented above. The slightly higher $K_{1/2}$ may result from less than 100% active Bms1 (see also Materials and Methods). In contrast, in the absence of Rcl1 and U3, the rate constant for GTP hydrolysis does not level off at the highest concentrations used (Figure 2(b)). This observation further confirms the cooperativity in binding of GTP, Rcl1 and U3 snoRNA to Bms1. Additionally, comparison of the absolute rates of GTP hydrolysis suggest that binding of U3 snoRNA and Rcl1 inhibit GTP hydrolysis of Bms1. While we do not understand the origin of this effect, it is tempting to speculate that it allows for further temporal control of the GTP hydrolysis of Bms1;[7] e.g. GTP hydrolysis could be inhibited until Bms1 interacts with the pre-ribosomal particle, or even with a specific conformation of the pre-ribosomal particle.

### Binding of Rcl1 to Bms1 and Bms1·U3

To determine whether there is thermodynamic coupling in the binding of U3 snoRNA and Rcl1, we wanted to determine the affinity of Bms1 for Rcl1 in the presence and in the absence of U3 snoRNA. Furthermore, determining the strength of the interaction between these two proteins provides insight into how Rcl1 release onto pre-ribosomes may be achieved. To measure the affinity between Bms1 and Rcl1, we took advantage of the observation that Rcl1 binding increases the affinity of Bms1 for GTP or GMPPNP as described above. We reasoned that at a concentration of GTP that is subsaturating in the absence of Rcl1, but close to saturating in the presence of Rcl1, addition of Rcl1 should increase the rate of GTP hydrolysis, because occupancy of Bms1 with GTP will be increased. To test this prediction and measure the affinity of Bms1 for Rcl1, we performed multiple-turnover experiments as described in Materials and Methods. The data show that addition of Rcl1 increases the observed rate constant for GTP hydrolysis with a $K_m$ value of 0.3 μM (Figure 3(a)).

We also determined the affinity of Bms1 for Rcl1 in single-turnover inhibition experiments. In these experiments, the affinity of Bms1 for GMPPNP was determined at different concentrations of Rcl1 and the resulting dependence of $K_i^{GMPPNP}$ on the Rcl1 concentration was fit to yield the $K_{1/2}$ for Rcl1 (Figure 3(b)), as described in Materials and Methods. The affinity for Rcl1 determined in this manner is 0.8 μM, very similar to the $K_m$ determined in the multiple-turnover experiments described above. The small difference in these values can be explained by the uncertainty in the $K_{1/2}$ determination, which was due to technical limitations at low concentrations of Bms1 and Rcl1, where the background GTPase rate was reached in the presence of the inhibitor GMPPNP. The similarity in the $K_m$ and $K_{1/2}$ values suggests that $K_m$ reflects $K_d$. This notion is further supported by the observation that binding of GTP and GDP is weak (Table 1), suggesting that product release is not likely to be rate-limiting. Furthermore, the $K_m$ value for GTP of 280 μM, determined in multiple-turnover experiments (Figure 4), is very similar to the $K_d$ value for GMPPNP, determined in single-turnover inhibition experiments, further suggesting that the $K_m$ value reflects the $K_d$ value without contributions from slow product release.

To confirm the observation that binding of Rcl1 increases the affinity of Bms1 for U3 snoRNA ($K_d$ = 1.0 μM and 0.6 μM in the absence and in the presence of Rcl1, respectively; Table 2), we determined the effect of addition of Rcl1 on GTP hydrolysis of the

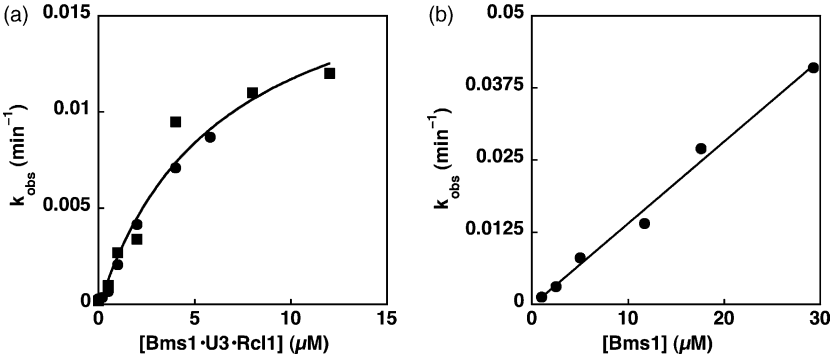


**Figure 2.** Single-turnover GTPase experiments. (a) GTP binding to the Bms1·Rcl1·U3 complex. Experiments were performed in the presence of 8.9 μM Rcl1 and twofold excess of U3 over Bms1 at all concentrations of U3. Circles and squares represent data from independent experiments. Both data sets were fit with equation (5) and yielded values of $K_d$ = 6 μM and $k_{max}$ = 0.19 min$^{-1}$. (b) GTP binding to Bms1. Experiments were performed at increasing concentrations of Bms1 with a trace of [γ-$^{32}$P]GTP.

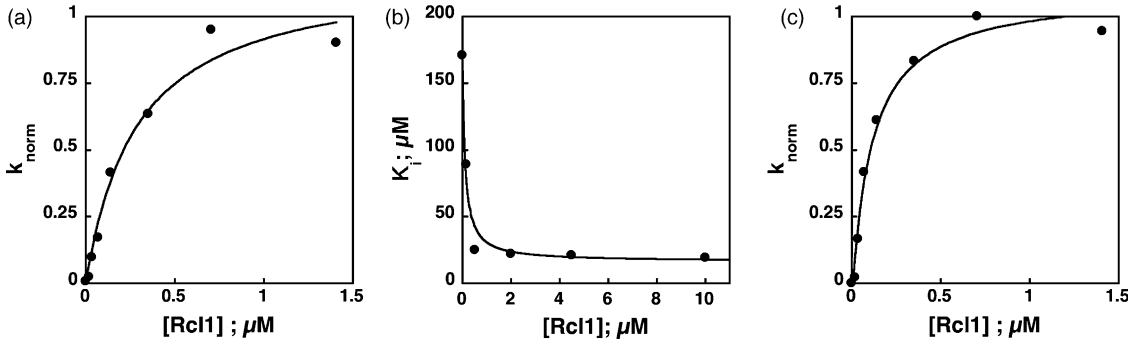


**Figure 3.** Rcl1 binding to Bms1. (a) Multiple-turnover experiments of Bms1 at increasing concentrations of Rcl1. Experiments were performed at 30 °C, 200 mM KCl, 10 mM $MgCl_2$ and 50 mM Hepes (pH 7.7). The concentration of Bms1 was 50 nM. Linear least-squares fitting of data to equation (6) yielded values of 0.3 μM for $K_m$. (b) Single-turnover experiments measuring the inhibition constant for GMPPNP at different concentrations of Rcl1. Experiments were performed at 30 °C, 200 mM KCl, 10 mM $MgCl_2$ and 50 mM Hepes (pH 7.7). Linear least-squares fitting to equation 4(c) yielded $K_{1/2}=0.8$ μM. (c) Multiple-turnover experiments of Bms1·U3 snoRNA at increasing concentrations of Rcl1. Experiments were performed at 30 °C, 200 mM KCl, 10 mM $MgCl_2$ and 50 mM Hepes (pH 7.7). The concentration of Bms1 was 50 nM and the concentration of U3 snoRNA was 4 μM. Linear least-squares fitting to equation (6) yielded $K_m=0.15$ μM.

Bms1·U3 complex. As shown in Figure 3(c), the $K_m$ for Rcl1 binding to Bms1·U3 is 0.1 μM, about threefold stronger than in the absence of U3 snoRNA, as expected from the RNA-binding experiments.

Taken together, these experiments indicate that there is a functional (and likely structural) linkage between the binding sites for U3 snoRNA and Rcl1 on Bms1. Furthermore, they show that binding of Bms1 to Rcl1 is tight, even in the absence of GTP.

## Discussion

### Bms1 assembles into thermodynamically well-behaved pre-ribosome subcomplexes

The essential GTPase Bms1, its putative endonuclease partner Rcl1 and U3 snoRNA form a subcomplex within the large processing complex responsible for biogenesis of the 40 S ribosomal subunit.[3,5–7] To test the thermodynamic stability and internal consistency of the Bms1 subcomplex assembly, we carried out a complete quantitative analysis of the formation of this subcomplex in the presence of GDP and the non-hydrolyzable GTP analog GMPPNP. These thermodynamic measurements were obtained using binding experiments in which the affinity for U3 snoRNA for different Bms1-containing complexes was assessed, and using GTP hydrolysis assays. In the latter, we determined binding constants for GDP and GMPPNP in inhibition experiments, as well as directly from GTPase rates as a function of increasing concentration of Bms1. Taken together, these data provide a quantitative description of ligand binding to Bms1 in the presence of GDP and GMPPNP, respectively (Figure 5(a) and (b)).

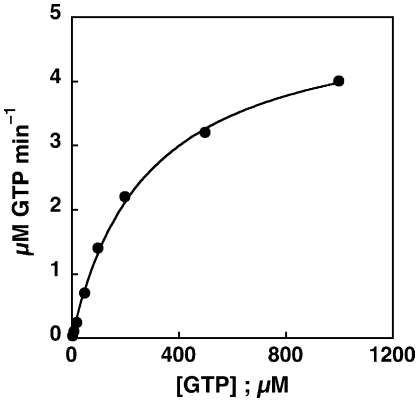


**Figure 4.** Multiple-turnover GTPase experiments. Experiments were performed at 30 °C, 200 mM KCl, 10 mM $MgCl_2$ and 50 mM Hepes (pH 7.7) in the presence of 1.4 μM Bms1. GTP at the indicated concentrations was spiked with [γ-$^{32}$P]GTP. Data were fit with equation (6) and yielded values of $K_m=280$ μM and $v_{max}=5.1$ μM GTP hydrolyzed $min^{-1}$.

The internal consistency, and thereby the quality of the data, can be assessed using the thermodynamic relationships within each side of the thermodynamic boxes in Figure 5(a) and (b). Because the free energy for formation of the ternary complex Bms1·U3·GDP relative to the free components Bms1+U3+GDP is independent of the order in which it is assembled, the product of the binding affinities must also be the same (equation (1); Scheme 1):

$$K_d^{U3} \bullet K_d^{GDP*} = K_d^{U3*} \bullet K_d^{GDP} \quad (1)$$

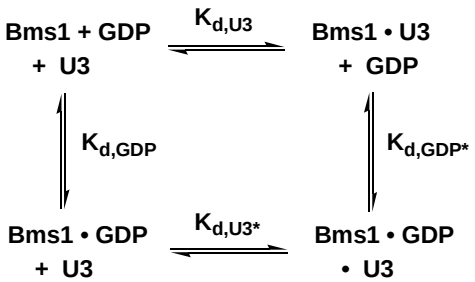


**Scheme 1.**

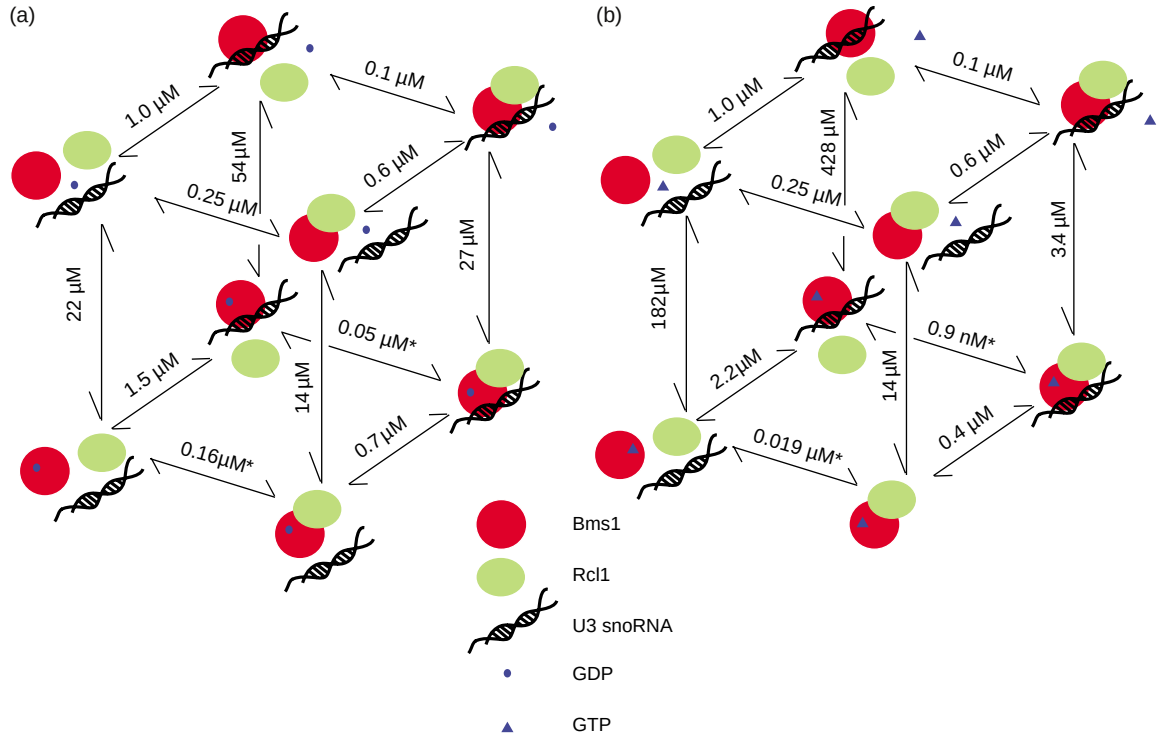


**Figure 5.** Thermodynamic cubes describing binding of Rcl1 and U3 snoRNA to Bms1 in the presence of (a) GDP or (b) the non-hydrolyzable GTP analog GMPPNP. Values marked with asterisks (*) are calculated from the thermodynamic relationships described by equation (7).

Scheme 1 and equation (1) can be applied to each side of the cubes in Figure 5. This analysis shows that the values within the GDP cube in Figure 5(a) are consistent within less than twofold (1.5–1.7-fold). For the GMPPNP box (Figure 5(b)) similar internal consistency is found (1.1–2.7-fold). This level of consistency is comparable to that observed for the well-characterized *Tetrahymena* group I ribozyme binding to its guanosine substrate and 5′-splice site analog, for the DEAD box helicase eIF4A binding to RNA and ATP, for eIF1 and eIF1A binding to ribosomes and for eIF2 binding to GTP and Met-tRNA (less than twofold).[10,30,33–36] These systems are also simpler, as they include only three components rather than four as in the Bms1·Rcl1·U3·GDP(GTP) complexes examined here. This level of internal consistency independently confirms values obtained in GTPase and RNA-binding experiments. The framework for formation of the Bms1·Rcl1·U3·nucleotide subcomplexes described here provides the basis to elucidate the function of additional factors in ribosome biogenesis that interact with this subcomplex during assembly of pre-ribosomes. This study is thus an important first step towards a more complete thermodynamic and functional description of the ribosome biogenesis apparatus.

## Release of Rcl1 onto pre-ribosomes is controlled kinetically

We have previously shown that Bms1 uses the cooperative interactions described here to deposit Rcl1 onto pre-ribosomes in a GTP-dependent manner.[7] In this model, Rcl1 is bound to Bms1 in the presence of GTP and U3 snoRNA, and will be released upon GTP hydrolysis. Here, we find that the affinity of Bms1 for Rcl1 is strong, with a dissociation constant of 0.3 μM, even in the absence of nucleotide. The concentration of Rcl1 *in vivo* is ~10 μM (K.K., S. Jonas & J.A.D., unpublished results)[37] and glycerol gradient analysis shows that most Rcl1 floats on top of the gradient, and is not associated with Bms1 or pre-ribosomes.[7] Thus, at equilibrium, Bms1 and Rcl1 are expected to be in a complex, regardless of the nucleotide-bound state of Bms1 (GTP or GDP). However, the strong affinity between Bms1 and Rcl1 will lead to slow dissociation of this complex. Assuming an association rate constant of $10^6$–$10^7$ $M^{-1}$ $s^{-1}$, typical of protein–protein association rate constants,[38] we can calculate dissociation rate constants from the measured $K_d$ values of 0.3 μM and 0.9 nM for free Bms1 and Bms1·GTP·U3, respectively. This calculation gives rate constants for Rcl1 dissociation of 0.3 $s^{-1}$–3 $s^{-1}$ and 0.0009 $s^{-1}$–0.009 $s^{-1}$, respectively, resulting in half-lifetimes of Rcl1 on Bms1 of 0.2–2 s for free Bms1 and 0.3–3 min for Bms1·GTP·U3. This suggests that release of Rcl1 from Bms1 or Bms1·GDP is rapid, while release of Rcl1 from the Bms1·GTP·U3 complex does not occur on the timescale of ribosome biogenesis *in vivo*. Thus, if Rcl1 release from Bms1 is irreversible, e.g. because rebinding is prevented by dissociation of Bms1 (Rcl1 needs Bms1 for binding to pre-ribosomes)[7] or

by trapping of Rcl1, the release of Rcl1 from Bms1 may be governed kinetically.

### Bms1 binding to Rcl1 is required for preferential binding of GTP over GDP

Bms1 binds GDP about eightfold more strongly than GTP; coupled with the approximately eightfold higher concentration of GTP over GDP *in vivo*, this means that only ~50% of Bms1 is in the activated, GTP-bound form. In contrast, when Rcl1 is bound, the binding affinity of Bms1 for GTP and GDP is essentially the same, thereby shifting the GTP occupancy to ~90%. Thus, Rcl1 promotes nucleotide exchange on Bms1, not by accelerating dissociation of GDP, but by favoring the GTP-bound form over the GDP-bound form. Rcl1 therefore helps to activate Bms1.

Similarly, recent data suggest that GDP/GTP exchange on the translation factor EF-G may be promoted by the ribosome *via* a thermodynamic effect.[15] The same appears to be true for translation initiation factor IF2.[9] For peptide release factor RF3, the ribosome has been shown to accelerate release of GDP and strengthen GTP binding.[14] These results suggest that for GTPases involved in translation, GDP affinity exceeds that for GTP, with this ratio being reversed upon effector binding (Table 3). Thus, the effectors of translational GTPases help to activate them. Interestingly, and in contrast to other GTPases, Bms1 shares this property with GTPases that are involved directly in translation. Similarly, analysis of the primary structure of Bms1 suggests that Bms1 is more closely related to GTPases involved in translation than to other GTPases.[5,39] Taken together, these observations imply that Bms1 evolved from translation factors, providing further evidence for adaptation of the translational machinery for ribosome biogenesis.[7]

In general, the GTPases that function as timing devices (Ras, EF-Tu) have guanosine exchange factors (GEFs) and guanosine-activating proteins (GAPs) to allow for a controlled time of action. In contrast, GTPases whose function is to render a reversible step irreversible (EF-G, RF3, Bms1), thereby conferring directionality to inherently equilibrated processes, do not have GEFs. The latter class may be especially useful in "cyclic" processes, where factors bind and later dissociate in a coordinated manner, such as translation and ribosome biogenesis. Such processes require energy to drive them forward. If Rcl1 binding to pre-ribosomes was stable, it would not dissociate, unless there was a change in the pre-ribosomes. Such a change could be brought about by RNA cleavage steps, which will release the energy stored in the phosphodiester bond, or by conformational changes, which require energy input. Alternatively, or additionally, Rcl1 may not bind stably to pre-ribosomes, therefore making dissociation irreversible, but remain bound long enough for its function to be completed once delivered there *via* the GTP-dependent activity of Bms1.

Intriguing similarities exist between Bms1 and the GTPases involved in translation with regard to the thermodynamics of nucleotide binding and the coupling of nucleotide and effector binding. All of these translational GTPases appear to bind to a similar site on the large ribosomal subunit,[17–19] where their GTPase activity is specifically activated. These observations suggest the possibility that Bms1 also interacts with this site on the large subunit, despite its involvement in 40 S but not 60 S biogenesis. This would allow for an integration of 40 S and 60 S biogenesis. However, we have shown elsewhere that, in contrast to the translational GTPases, Bms1 has an internal GAP domain,[7] which provides a modest amount of stimulation for its GAP activity. In contrast, the translational GTPases are activated $>10^4$ fold by the ribosome (see Table S1 of Karbstein et al.[7] and references therein). Thus, Bms1 may differ from the translational GTPases in its mechanism of activation, possibly because of its involvement in an early step in ribosome biogenesis when the GAP center on the ribosome is not yet formed.

**Table 3.** GTP and GDP affinities for different GTPases

| | Free protein | | | Effector complex | | | |
|---|---|---|---|---|---|---|---|
| Protein | $K_d^{GTP}$ | $K_d^{GDP}$ | Ratio | $K_d^{GTP}$ | $K_d^{GDP}$ | Ratio | Reference |
| Bms1 | 182 μM | 22 μM | 8.3 | 3.4 μM | 27 μM | 0.13 | This work, 7 |
| EF-G | >600 μM | 13 μM | >50 | | | 0.0063 | 15 |
| EF-Tu | 60 nM | 1 nM | 60 | 14 nM[a] | 9 nM[a] | 1.6[a] | 11 |
| | | | | | | 0.01[b] | 12,13,16 |
| IF2 | >>20 μM | 7 μM | >>3 | 2 μM | 7 μM | 0.3 | 9 |
| RF3 | 2.5 μM | 5.5 nM | 450 | 39 nM | | | 14 |
| FtsY | 14 μM | 26 μM | 0.5 | | | | 40 |
| Ffh | 0.3 μM | 0.2 μM | 1.5 | | | | 40 |
| Ras | 0.7 pM | 8 pM | 0.09 | | | | 44 |
| Sec4 | 3.4 nM | 77 nM | 0.04 | | | | 45 |

[a] In the presence of EF-Ts.
[b] In the presence of tRNA.

## Materials and Methods

### Materials

GTP, GMPPNP and GDP were purchased from Sigma and purified by fast protein liquid chromatography (FPLC) by anion-exchange using a Mono Q column (Amersham). Nucleotides were bound in 50 mM $(NH_4)HCO_3$ (pH 8.0) and eluted with a salt gradient to 1 M $(NH_4)HCO_3$. Peak fractions were lyophilized twice and analyzed for purity on a thin-layer chromatography (TLC) plate. No contaminations were observed. Nucleotides were dissolved in water and aliquots were flash-frozen and stored at −80 °C. [$\gamma$-$^{32}$P]GTP was purchased from Amersham, purified on a 24% polyacrylamide/TBE gel, eluted overnight with water and stored at −20 °C.

### Transcriptions

Transcriptions were performed in the presence of 40 mM Tris–HCl (pH 8.1), 25 mM $MgCl_2$, 2 mM spermidine, 0.01% (v/v) Triton X-100, 2 mM each NTP, 40 mM DTT, 0.5 mg of phage T7 RNA polymerase and 200 μg of template/10 ml reaction, as described.[7] Following transcription, RNA was purified using RNeasy columns (Qiagen) or *via* gel-purification. No functional difference was observed between these two preparations. Radioactively labeled RNA was obtained by transcriptions in the presence of [$\alpha$-$^{32}$P]ATP (Amersham), essentially as described above, except that 0.2 mM ATP and 1 μg of template/50 μl reaction was used. Transcripts were purified on a 6% polyacrylamide/TBE gel in the presence of 8 M urea. RNA was eluted from the gel using an Elutrap gel-electroelution device (Schleicher&Schuell) and stored in TBE at −20 °C.

### Protein expression and purification

Bms1 protein was produced in Rosetta cells (Novagen) as described.[7] Rcl1 was produced in BL21(DE3) cells as described.[7] Cells were grown at 37 °C to an absorbance of 0.4, at 600 nm induced by addition of IPTG to a concentration of 0.1 mM and shifted to 30 °C, where they were grown for 4 h prior to harvest.

Bms1 protein was purified as described.[7] Briefly, after resuspension in buffer A (50 mM $NaH_2PO_4$ (pH 8.0), 300 mM NaCl, 1 M KCl, 2 mM EDTA) supplemented with 0.5 mM PMSF and two tablets of protease, inhibitor cells were lysed and the cleared lysate was loaded onto a gravity-flow column with 4 ml of amylose resin (New England Biolabs). Protein was eluted in buffer B (50 mM $NaH_2PO_4$ (pH 8.0), 300 mM NaCl, 10 mM maltose, 2 mM EDTA) and concentrated for loading onto a Superdex 200 column. The gel-filtration chromatography column was run in 200 mM KCl, 50 mM Hepes (pH 7.7), 1 mM DTT, 1 mM Tris(2-carboxyethyl)phosphine hydrochloride (TCEP) and Bms1-containing fractions were pooled and concentrated. Purity was >98% as judged from SDS-PAGE analysis. Protein was stored at 4 °C for two to three weeks. Previous work has shown that GTPase and RNA-binding activities arise from Bms1 and not a contaminant in the purification.[7]

Rcl1 was purified as described,[7] with the addition of a 1 ml of Blue-Sepharose (Amersham) column prior to gel-filtration. Briefly, cell lysate was loaded at 1 ml/min onto a 5 ml Fast-flow S column (Amersham). Protein was eluted in a salt gradient to 1 M NaCl over ten column volumes. Rcl1-containing fractions were pooled, diluted twofold and loaded onto the Blue-Sepharose column, eluted in a gradient to 1 M NaCl over 15 column volumes and concentrated for injection onto a Superdex 75 column. No visible contamination was observed by SDS-PAGE.[7] Protein was flash-frozen in liquid nitrogen for long-term storage at −80 °C, where it is stable for at least one year.

Protein concentrations were determined by the Bradford method using a bovine serum albumin (BSA) standard curve.

Rcl1 and Bms1 binding assays were used to determine the fraction of active molecules. Assuming a 1:1 stoichiometry, these experiments suggest that >90% of Rcl1 molecules are active and >60% of Bms1 molecules are active in these protein preparations (data not shown).

### General kinetic methods

GTPase assays were performed at 30 °C in the presence of 10 mM $MgCl_2$, 200 mM KCl, 50 mM Hepes (pH 7.7). Samples were taken at specified time-points and quenched by addition of an equal volume of 0.75 M $KH_2PO_4$ (pH 3.3);[40] 1 μl of the quenched reaction was spotted onto a PEI-F cellulose TLC plate (JT Baker or EMD Biosciences), which had been washed with 10% (w/v) NaCl and then twice with water.[7] The TLC plate was developed in 1 M LiCl, 300 mM $NaH_2PO_4$ pH (3.8)[7,40] and exposed to a phosphoscreen for Phosphorimager quantification. The spots corresponding to remaining [$\gamma$-$^{32}$P]GTP and to appearing [$^{32}$P]phosphate were quantified separately, and fractions of reacted material were determined. These were fit to equation (2) by a linear least-squares procedure to obtain rate constants $k_{obs}$ for GTP hydrolysis:

$$\text{fraction}_{\text{reacted}} = \text{fraction}^{\max}_{\text{reacted}} - \text{fraction}^{\max}_{\text{reacted}} \bullet \exp(-k_{\text{obs}} \bullet t) \quad (2)$$

For multiple-turnover experiments, only the initial linear portion of the graph ($\leq$15%) was fit, assuming an endpoint of 95% (as observed in single-turnover reactions). This was done to ensure that inhibition from the GDP product did not affect the observed rate constant.

### $K_i$ values

Inhibition constants for GDP and GMPPNP were obtained in single-turnover experiments. In these experiments, a trace amount (<1 nM) of [$\gamma$-$^{32}$P]GTP was added to subsaturating concentrations of Bms1 and increasing concentrations of GDP or GMPPNP. At concentrations greater than 1 mM, an equal concentration of $MgCl_2$ was added to the reaction to account for chelation of $Mg^{2+}$ by the nucleotide. The data were fit with equation (3) (which holds only when Bms1 is subaturating with respect to GTP) to obtain $K_i$. Here, $k_{max}$ is the rate constant in the absence of GDP or GMPPNP and $k_{obs}$ is the rate constant in the presence of a given concentration of GDP or GMPPNP.

$$k_{\text{obs}} = \frac{k_{\max}}{1 + \frac{[\text{GDP}]}{K_i}} \quad (3)$$

Reactions in the presence of U3 RNA were performed with U3 RNA concentrations in at least twofold excess of Bms1 and at saturating concentrations to ensure that all Bms1 has U3 RNA bound.

To determine the affinity of Rcl1 $K_i^{\text{GMPPNP}}$ values were measured as a function of the concentration of Rcl1. The

data were fit with equation (4c), derived from equation (4a), where $K_a$ values represent association constants and $K_i$ values represent dissociation constants. $K_{i,obs}^{GMPPNP}$ is the measured affinity of GMPPNP at a given concentration of Rcl1, $K_{i,Bms1}^{GMPPNP}$ is the affinity of GMPPNP for free Bms1, $K_{i,Bms1\bullet Rcl1}^{GMPPNP}$ is the affinity of GMPPNP for the Bms1·Rcl1 complex and $K_d^{Rcl1}$ is the affinity of Rcl1 for Bms1:

$$K_{a,obs}^{GMPPNP} = K_{a,Bms1}^{GMPPNP}\frac{K_d^{Rcl1*}}{K_d^{Rcl1*} + [Rcl1]_{total}} + K_{a,Bms1\bullet Rcl1}^{GMPPNP}\left(\frac{[Rcl1]}{K_d^{Rcl1*} + [Rcl1]_{total}}\right) \quad (4a)$$

$$K_d^{Rcl1*} = K_d^{Rcl1} + [Bms1] \quad (4b)$$

$$K_{i,obs}^{GMPPNP} = \frac{K_{i,Bms1}^{GMPPNP}\bullet K_{i,Bms1\bullet Rcl1}^{GMPPNP}\bullet(K_d^{Rcl1*} + [Rcl1])}{K_{i,Bms1}^{GMPPNP}\bullet[Rcl1] + K_{i,Bms1\bullet Rcl1}^{GMPPNP}\bullet K_d^{Rcl1*}} \quad (4c)$$

The modification of equation (4b) takes into account that, for technical reasons, it was not possible to keep the concentration of Bms1 below the concentration of Rcl1 when low concentrations of Rcl1 were used. This is because the limit of background GTPase rate was reached in the presence of GMPPNP inhibitor.

### Multiple-turnover experiments to determine the affinity of Bms1 for Rcl1

The affinity of Rcl1 for Bms1, $K_d^{Rcl1}$, was determined in multiple-turnover experiments using 20 μM GTP, doped with [γ-$^{32}$P]GTP, 50 nM Bms1 and increasing concentrations of Rcl1. Assuming an endpoint of 95% (as observed in single-turnover reactions) the initial linear portion of the graph was fit with equation (2) to obtain $k_{obs}$ values. In parallel reactions, the observed rate constant for GTP hydrolysis in the absence of Bms1 was measured to eliminate the contribution from a very minor GTPase contaminant in Rcl1. The rate constants from these control reactions were subtracted from the $k_{obs}$ values to obtain $k'_{obs}$ values. These were plotted against the Rcl1 concentrations at which they were obtained, and fit with equation (5) to obtain the values for the affinity of Rcl1 for Bms1:

$$k'_{obs} = k'_{max}\frac{[Rcl1]}{[Rcl1] + K_d^{Rcl1}} \quad (5)$$

This treatment assumes that the rate constants for association and dissociation of Rcl1 are fast relative to GTP hydrolysis (otherwise $K_m$ has no relationship to $K_d$). Assuming a second-order association rate constant of $10^6$–$10^7$ $M^{-1}$ $s^{-1}$, typical of protein–protein association rate constants,[38] we can calculate an association rate constant of $>6$ $min^{-1}$ at 100 nM Rcl1 and a dissociation rate constant of $>18$ $min^{-1}$. This is rapid relative to the slow GTP hydrolysis of Bms1 of 0.01 $min^{-1}$ (Figure 2(a)). Additionally, equation (5) was derived with the simplification that GTP hydrolysis by Bms1 is negligible relative to hydrolysis by Bms1·Rcl1. Given the approximately tenfold effect of Rcl1 on GTP binding, this simplification appears valid. Note also that the stimulation of the GTPase rate arises because of the difference in GTP binding of Bms1 and Bms1·Rcl1.

### $K_m^{GTP}$ values from multiple-turnover experiments

$K_m^{GTP}$ values were determined in the presence of 0.5–1.5 μM Bms1 and increasing concentrations of GTP, doped with trace amounts of [γ-$^{32}$P]GTP. The linear initial portion of the graph was fit with equation (2), as described above, to yield $k_{obs}$ values, which were multiplied by the concentration of GTP at which they were obtained, to yield rates. Rates were plotted against the concentration of GTP at which they were obtained, and fit with equation (6) to obtain $K_m^{GTP}$ values:

$$v_{obs} = v_{max}\frac{[GTP]}{[GTP] + K_m^{GTP}} \quad (6)$$

### Filter-binding assays

U3 snoRNA was prefolded by incubating it for 20 min at 55 °C in the presence of 10 mM $MgCl_2$ and 50 mM Hepes (pH 7.7). After this preincubation, the RNA ran as a single band in native polyacrylamide gels and was able to bind Bms1 protein. After folding, U3 snoRNA was incubated for 2–3 h with Bms1 protein at 30 °C in the presence of binding buffer (10 mM $MgCl_2$, 50 mM Hepes (pH 7.7) and 200 mM KCl). During incubation, the membranes for filter-binding [Hybond-N, Hybond-ECF (both Amersham) and Tuffryn 0.45 μm pore size filters (Pall Corporation)] were washed for 30 min in binding buffer and then assembled in the filter-binding device. The vacuum was turned on and the reactions were spotted onto the membranes, taking caution not to touch the top membrane. After all reactions were spotted, each spot was washed with 100 μl of binding buffer. After all liquid was filtered, membranes were disassembled and exposed to a phosphoscreen. Bound and free RNA were quantified and the fraction of bound RNA was fit by linear least-squares fitting with equation (7) to obtain $K_d$ values:

$$\text{fraction}_{bound} = \text{fraction}_{bound}^{max}\frac{[Bms1]}{[Bms1] + K_d} \quad (7)$$

## Acknowledgements

This work was supported, in part, by NIH grant GM22778. J.A.D. is an investigator of the Howard Hughes Medical Institute. K.K. is a Damon Runyon Fellow supported by the Damon Runyon Cancer Research Foundation (DRG-1807-04). We thank S. Shan for helpful discussion and K. Carroll, C. Fraser, D. Herschlag, J. Kirsch and I. McRae for comments on the manuscript.

## References

1. Fromont-Racine, M., Senger, B., Saveanu, C. & Fasiolo, F. (2003). Ribosome assembly in eukaryotes. *Gene*, **313**, 17–42.
2. Dragon, F., Gallagher, J. E., Compagnone-Post, P. A., Mitchell, B. M., Porwancher, K. A., Wehner, K. A. *et al.* (2002). A large nucleolar U3 ribonucleoprotein required for 18 S ribosomal RNA biogenesis. *Nature*, **417**, 967–970.
3. Grandi, P., Rybin, V., Bassler, J., Petfalski, E., Strauss, D., Marzioch, M. *et al.* (2002). 90S pre-ribosomes include the

35S pre-rRNA, the U3 snoRNP, and 40 S subunit processing factors but predominantly lack 60 S synthesis factors. *Mol. Cell*, **10**, 105–115.
4. Gelperin, D., Horton, L., Beckman, J., Hensold, J. & Lemmon, S. K. (2001). Bms1p, a novel GTP-binding protein, and the related Tsr1p are required for distinct steps of 40 S ribosome biogenesis in yeast. *RNA*, **7**, 1268–1283.
5. Wegierski, T., Billy, E., Nasr, F. & Filipowicz, W. (2001). Bms1p, a G-domain-containing protein, associates with Rcl1p and is required for 18 S rRNA biogenesis in yeast. *RNA*, **7**, 1254–1267.
6. Krogan, N. J., Peng, W. T., Cagney, G., Robinson, M. D., Haw, R., Zhong, G. *et al*. (2004). High-definition macromolecular composition of yeast RNA-processing complexes. *Mol. Cell*, **13**, 225–239.
7. Karbstein, K., Jonas, S. & Doudna, J. A. (2005). An essential GTPase promotes assembly of pre-ribosomal processing complexes. *Mol. Cell*, **20**, 633–643.
8. Bourne, H. R., Sanders, D. A. & McCormick, F. (1991). The GTPase superfamily: conserved structure and molecular mechanism. *Nature*, **349**, 117–127.
9. Antoun, A., Pavlov, M. Y., Andersson, K., Tenson, T. & Ehrenberg, M. (2003). The roles of initiation factor 2 and guanosine triphosphate in initiation of protein synthesis. *EMBO J.* **22**, 5593–5601.
10. Kapp, L. D. & Lorsch, J. R. (2004). GTP-dependent recognition of the methionine moiety on initiator tRNA by translation factor eIF2. *J. Mol. Biol.* **335**, 923–936.
11. Gromadski, K. B., Wieden, H. J. & Rodnina, M. V. (2002). Kinetic mechanism of elongation factor Ts-catalyzed nucleotide exchange in elongation factor Tu. *Biochemistry*, **41**, 162–169.
12. Pingoud, A., Block, W., Wittinghofer, A., Wolf, H. & Fischer, E. (1982). The elongation factor Tu binds aminoacyl-tRNA in the presence of GDP. *J. Biol. Chem.* **257**, 11261–11267.
13. Pingoud, A. & Urbanke, C. (1980). Aminoacyl transfer ribonucleic acid binding site of the bacterial elongation factor Tu. *Biochemistry*, **19**, 2108–2112.
14. Zavialov, A. V., Buckingham, R. H. & Ehrenberg, M. (2001). A posttermination ribosomal complex is the guanine nucleotide exchange factor for peptide release factor RF3. *Cell*, **107**, 115–124.
15. Zavialov, A. V., Hauryliuk, V. V. & Ehrenberg, M. (2005). Guanine-nucleotide exchange on ribosome-bound elongation factor G initiates the translocation of tRNAs. *J. Biol.* **4**, 9.
16. Romero, G., Chau, V. & Biltonen, R. L. (1985). Kinetics and thermodynamics of the interaction of elongation factor Tu with elongation factor Ts, guanine nucleotides, and aminoacyl-tRNA. *J. Biol. Chem.* **260**, 6167–6174.
17. Moazed, D., Robertson, J. M. & Noller, H. F. (1988). Interaction of elongation factors EF-G and EF-Tu with a conserved loop in 23 S RNA. *Nature*, **334**, 362–364.
18. Klaholz, B. P., Myasnikov, A. G. & Van Heel, M. (2004). Visualization of release factor 3 on the ribosome during termination of protein synthesis. *Nature*, **427**, 862–865.
19. Allen, G. S., Zavialov, A., Gursky, R., Ehrenberg, M. & Frank, J. (2005). The cryo-EM structure of a translation initiation complex from *Escherichia coli*. *Cell*, **121**, 703–712.
20. Rodnina, M. V., Savelsbergh, A., Katunin, V. I. & Wintermeyer, W. (1997). Hydrolysis of GTP by elongation factor G drives tRNA movement on the ribosome. *Nature*, **385**, 37–41.
21. Pape, T., Wintermeyer, W. & Rodnina, M. V. (1998). Complete kinetic mechanism of elongation factor Tu-dependent binding of aminoacyl-tRNA to the A site of the *E. coli* ribosome. *EMBO J.* **17**, 7490–7497.
22. Parmeggiani, A. & Sander, G. (1981). Properties and regulation of the GTPase activities of elongation factors Tu and G, and of initiation factor 2. *Mol. Cell. Biochem.* **35**, 129–158.
23. Tomsic, J., Vitali, L. A., Daviter, T., Savelsbergh, A., Spurio, R., Striebeck, P. *et al*. (2000). Late events of translation initiation in bacteria: a kinetic analysis. *EMBO J.* **19**, 2127–2136.
24. Shan, S. O. & Walter, P. (2003). Induced nucleotide specificity in a GTPase. *Proc. Natl Acad. Sci. USA*, **100**, 4480–4485.
25. Shan, S., Kravchuk, A. V., Piccirilli, J. A. & Herschlag, D. (2001). Defining the catalytic metal ion interactions in the Tetrahymena ribozyme reaction. *Biochemistry*, **40**, 5161–5171.
26. Shan, S. O., Narlikar, G. J. & Herschlag, D. (1999). Protonated 2′-aminoguanosine as a probe of the electrostatic environment of the active site of the Tetrahymena group I ribozyme. *Biochemistry*, **38**, 10976–10988.
27. Ortoleva-Donnelly, L., Kronman, M. & Strobel, S. A. (1998). Identifying RNA minor groove tertiary contacts by nucleotide analogue interference mapping with N-2-methylguanosine. *Biochemistry*, **37**, 12933–12942.
28. Szewczak, A. A., Ortolevadonnelly, L., Ryder, S. P., Moncoeur, E. & Strobel, S. A. (1998). A minor-groove RNA triple-helix within the catalytic core of a group I intron. *Nature Struct. Biol.* **5**, 1037–1042.
29. Karbstein, K., Tang, K. H. & Herschlag, D. (2004). A base triple in the Tetrahymena group I core affects the reaction equilibrium *via* a threshold effect. *RNA*, **10**, 1730–1739.
30. Knitt, D. S., Narlikar, G. J. & Herschlag, D. (1994). Dissection of the role of the conserved G.U pair in group I RNA self-splicing. *Biochemistry*, **33**, 13864–13879.
31. Peluso, P., Herschlag, D., Nock, S., Freymann, D. M., Johnson, A. E. & Walter, P. (2000). Role of 4.5 S RNA in assembly of the bacterial signal recognition particle with its receptor. *Science*, **288**, 1640–1643.
32. Shan, S. O. & Walter, P. (2005). Molecular crosstalk between the nucleotide specificity determinant of the SRP GTPase and the SRP receptor. *Biochemistry*, **44**, 6214–6222.
33. Maag, D. & Lorsch, J. R. (2003). Communication between eukaryotic translation initiation factors 1 and 1A on the yeast small ribosomal subunit. *J. Mol. Biol.* **330**, 917–924.
34. Vetter, I. R. & Wittinghofer, A. (2001). The guanine nucleotide-binding switch in three dimensions. *Science*, **294**, 1299–1304.
35. Karbstein, K., Carroll, K. S. & Herschlag, D. (2002). Probing the Tetrahymena group I ribozyme reaction in both directions. *Biochemistry*, **41**, 11171–11183.
36. Lorsch, J. R. & Herschlag, D. (1998). The DEAD box protein eIF4A 1. A minimal kinetic and thermodynamic framework reveals coupled binding of RNA and nucleotide. *Biochemistry*, **37**, 2180–2193.
37. Ghaemmaghami, S., Huh, W. K., Bower, K., Howson, R. W., Belle, A., Dephoure, N. *et al*. (2003). Global analysis of protein expression in yeast. *Nature*, **425**, 737–741.
38. Fersht, A. (1984). *Enzyme Structure and Mechanism*, W.H. Freeman & Company, New York.

39. Sanchez, R. & Sali, A. (1998). Large-scale protein structure modeling of the Saccharomyces cerevisiae genome. *Proc. Natl Acad. Sci. USA*, **95**, 13597–13602.
40. Peluso, P., Shan, S. O., Nock, S., Herschlag, D. & Walter, P. (2001). Role of SRP RNA in the GTPase cycles of Ffh and FtsY. *Biochemistry*, **40**, 15224–15233.
41. Venema, J. & Tollervey, D. (1999). Ribosome synthesis in *Saccharomyces cerevisiae*. *Annu. Rev. Genet.* **33**, 261–311.
42. Billy, E., Wegierski, T., Nasr, F. & Filipowicz, W. (2000). Rcl1p, the yeast protein similar to the RNA 3′-phosphate cyclase, associates with U3 snoRNP and is required for 18 S rRNA biogenesis. *EMBO J.* **19**, 2115–2126.
43. van Hoof, A., Lennertz, P. & Parker, R. (2000). Three conserved members of the RNase D family have unique and overlapping functions in the processing of 5 S, 5.8 S, U4, U5, RNase MRP and RNase P RNAs in yeast. *EMBO J.* **19**, 1357–1365.
44. Neal, S. E., Eccleston, J. F., Hall, A. & Webb, M. R. (1988). Kinetic analysis of the hydrolysis of GTP by p21N-ras. The basal GTPase mechanism. *J. Biol. Chem.* **263**, 19718–19722.
45. Kabcenell, A. K., Goud, B., Northup, J. K. & Novick, P. J. (1990). Binding and hydrolysis of guanine nucleotides by Sec4p, a yeast protein involved in the regulation of vesicular traffic. *J. Biol. Chem.* **265**, 9366–9372.

***Edited by D. E. Draper***

*(Received 15 September 2005; received in revised form 15 November 2005; accepted 16 November 2005)*
Available online 5 December 2005